ASTROBIOLOGY
Volume 9, Number 7, 2009

DOI: 10.1089/ast.2008.0324

Research Article

Formation of Uracil from the Ultraviolet Photo-Irradiation of Pyrimidine in Pure H_2O Ices

Michel Nuevo,[1] Stefanie N. Milam,[1,2] Scott A. Sandford,[1] Jamie E. Elsila,[3] and Jason P. Dworkin[3]

Abstract

The detection of nucleobases in carbonaceous chondrites such as Murchison supports the scenario in which extraterrestrial organic molecules could have contributed to the origin of life on Earth. However, such large molecules have not been observed to date in astrophysical environments, in particular, comets and the interstellar medium (ISM). The physico-chemical conditions under which nucleobases and, more generally, *N*-heterocycles were formed are unknown, as are their mechanisms of formation. In this work, H_2O:pyrimidine ice mixtures were irradiated with UV photons under interstellar/cometary–relevant conditions to study the formation of pyrimidine derivatives, including the nucleobase uracil. Liquid and gas chromatography analyses of the samples produced in our experiments revealed the presence of numerous photoproducts among which 4(3*H*)-pyrimidone and uracil could be conclusively identified. The photostability of pyrimidine against UV photons was also studied, and we showed that it would survive from the ISM to the solar nebula if formed and preserved in ice mantles on the surface of cold grains. We propose pathways for the formation of 4(3*H*)-pyrimidone and uracil under astrophysically relevant conditions and discuss the possibility for such molecules to survive from the ISM to their delivery to Earth and other Solar System bodies. Key Words: Pyrimidine—Nucleobases—Interstellar ices—Cometary ices—Molecular processes—Prebiotic chemistry. Astrobiology 9, 683–695.

1. Introduction

Nucleobases are the building blocks of RNA (ribonucleic acid) and DNA (deoxyribonucleic acid), the genetic material used by all living organisms on Earth. Their molecular structures are based on two *N*-heterocyclic aromatic compounds, namely, pyrimidine ($C_4H_4N_2$) and purine ($C_5H_4N_4$). Among the biological nucleobases, three are pyrimidine-based: uracil (found in RNA only), thymine (in DNA only), and cytosine (in both RNA and DNA); and two are purine-based: adenine and guanine (in both RNA and DNA). The molecular structures of pyrimidine, purine, and their derived nucleobases are given in Fig. 1.

N-heterocycles of prebiotic/biological interest have been extensively sought in extraterrestrial materials, particularly meteorites. Purines have been detected in the carbonaceous chondrites Murchison, Murray, and Orgueil (Hayatsu, 1964; Folsome *et al.*, 1971, 1973; Hayatsu *et al.*, 1975; van der Velden and Schwartz, 1977). In contrast, among biological pyrimidine-based compounds, only uracil has been confirmed in water and formic acid extracts of the same three carbonaceous meteorites (Stoks and Schwartz, 1979, 1981). The presence of the nucleobases uracil and xanthine (non-biological) has recently been confirmed in Murchison and their extraterrestrial origin established by their isotopic ratios (Martins *et al.*, 2008).

Nucleobases and other *N*-heterocycles have also been extensively sought throughout the interstellar medium (ISM), particularly in molecular clouds (Simon and Simon, 1973; Kuan *et al.*, 2003, 2004; Charnley *et al.*, 2005). However, *N*-heterocycles have yet to be detected in the ISM in the gas phase, where only upper limits of $1.7–3.4\times10^{14}\,cm^{-2}$ for the column densities of pyrimidine have been estimated (Kuan *et al.*, 2003). These observations, however, do not place constraints on the abundance of pyrimidine and its derivatives. Such compounds may be formed in the solid phase on the surface of cold interstellar grains or in meteorites' parent bodies (asteroids and comets) rather than in the gas phase.

Aromatic species, including polycyclic aromatic hydrocarbons (PAHs) and polycyclic aromatic nitrogen heterocycles (PANHs), are believed to be present in interstellar and circumstellar environments, where these gas-phase compounds

[1]NASA Ames Research Center, Space Science Division, Moffett Field, California.
[2]SETI Institute, Mountain View, California.
[3]NASA Goddard Space Flight Center, Solar System Exploration Division, Greenbelt, Maryland.

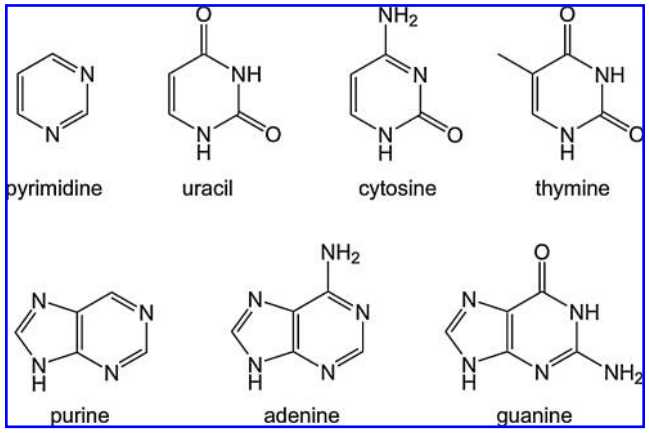

FIG. 1. Molecular structures of pyrimidine, purine, and the biological pyrimidine- and purine-based nucleobases uracil, cytosine, thymine, adenine, and guanine.

in their neutral and ionic forms are believed to produce strong infrared emission bands detected throughout our Galaxy (Allamandola *et al.*, 1989; Puget and Léger, 1989; Roelfsema *et al.*, 1996) and in other galaxies (see, *e.g.*, Galliano *et al.*, 2008). These complex species, which represent a large fraction (up to 17%) of the interstellar and circumstellar carbon (Allamandola *et al.*, 1989; Puget and Léger, 1989), could be formed, at least partly, from the polymerization of small molecules such as acetylene. The presence of *N*-bearing species such as HCN during this polymerization could allow nitrogen atoms to be incorporated into the aromatic rings to form compounds such as pyridine and pyrimidine (Ricca *et al.*, 2001). Additionally, gas-phase PAHs and PANHs are likely to condense onto the icy surfaces of cold grains in molecular clouds (Sandford *et al.*, 2004; Bernstein *et al.*, 2005), where they are likely involved in complex chemistry that occurs in these environments.

The presence of aromatic cyclic compounds in interstellar ices is of particular interest since it has been shown in the laboratory that radiation processing (UV photo-irradiation and proton bombardment) of PAHs in astrophysical ice analogues leads to the production of astrobiologically interesting products like quinones, ethers, and other functionalized aromatic species (Bernstein *et al.*, 1999, 2001, 2002b, 2003; Ashbourn *et al.*, 2007). However, relatively little work has been done on the radiation processing of PANHs in ices (Elsila *et al.*, 2006), even though these might also be expected to produce a host of molecules of astrobiological relevance.

In the present work, we report the UV photoprocessing of the *N*-heterocycle pyrimidine (Fig. 1) in H_2O-rich ices, focusing on the study of the formation of oxidized pyrimidine derivatives, including the nucleobase uracil, in the solid phase under interstellar and cometary conditions. For this, we explored several experimental parameters such as the relative proportion between H_2O and pyrimidine, the temperature of irradiation, and the UV photon wavelength. The astrobiological implications of these results are discussed with focus on the mechanisms of formation. We also established the photostability of pyrimidine-based compounds, including uracil, and discuss the likelihood of their delivery from the astrophysical environments where they may form to the surface of telluric planets such as primitive Earth.

2. Experimental Methods

2.1. UV photo-irradiation of H_2O:pyrimidine ices at low temperature

Sample preparation was carried out at NASA Ames Research Center inside a vacuum cryogenic chamber evacuated by a diffusion pump (Edwards BRV 25) to a pressure of a few 10^{-8} torr. H_2O:pyrimidine gas mixtures were deposited onto an aluminum (Al) foil, prebaked at 500°C, and attached to a cold finger cooled to 20–30 K by a closed-cycle helium cryocooler (APD Cryogenics) (Allamandola *et al.*, 1988; Bernstein *et al.*, 1995). These H_2O:pyrimidine gas mixtures were prepared in a glass line evacuated by a diffusion pump (Edwards BRV 10, background pressure $\sim 10^{-6}$ torr). H_2O (purified to an 18.2 MΩ cm resistivity by a Millipore Direct-Q UV 3 device, and freeze-pump-thawed four times to remove excess dissolved gases) and pyrimidine (Aldrich, 99% purity) were mixed in 2.1-liter glass bulbs, with the ratios between the two components determined by their partial pressure in the bulb (accurate to 0.05 mbar). In this work, H_2O:pyrimidine mixtures with relative proportions of 10:1, 20:1, 40:1, and 100:1 were prepared, with total pressures of $\sim$20 mbar in each bulb.

In a typical experiment, two identical $\sim$20 mbar bulbs were used, with a total of about 35–40 mbar ($\sim$2.9–3.4 mmol) deposited and condensed onto the cooled Al foil. Simultaneously with the deposition, the growing H_2O:pyrimidine ice layer was photo-irradiated with a microwave-powered H_2 discharge UV lamp (Opthos). This lamp emits photons mainly at 121.6 nm (Lyman α) and in a continuum centered around 160 nm, with an estimated total flux of $\sim 2\times10^{15}$ photons cm^{-2} s^{-1} (Bernstein *et al.*, 1999; Elsila *et al.*, 2007, and references therein), and simulates the UV radiation field found in many astrophysical environments. The temperature of deposition and the deposition/irradiation time were typically 20–30 K and 22–23 h, respectively.

A typical photon flux for diffuse interstellar environments is estimated to be 8×10^7 photons cm^{-2} s^{-1} for photons with energies higher than 6 eV (Mathis *et al.*, 1983). In more opaque dense interstellar clouds, fluxes are expected to be 3 (Shen *et al.*, 2004) to 5 (Prasad and Tarafdar, 1983) orders of magnitude lower. Our laboratory experiments, therefore, correspond to a UV photo-irradiation of ices for about 7×10^3 years in diffuse media, and $7\times10^{6-8}$ years in dense media.

After irradiation, the samples were warmed to 220 K in a static vacuum (*i.e.*, under vacuum but without active pumping) at a rate of 2–3 K min^{-1}, at which time the sample was removed from the vacuum chamber. The foil was then removed from the cold finger and put in a waiting vial that had been baked overnight in a muffle furnace at 450°C. Samples for high-performance liquid chromatography analysis at NASA Ames Research Center were dissolved in 500 μL of H_2O (18.2 MΩ cm resistivity, Millipore Direct-Q UV 3), whereas samples for gas chromatography–mass spectrometry analysis were kept dry in similar vials and shipped to NASA Goddard Space Flight Center for analysis. Although we present here only the data for one typical sample produced from the irradiation of an H_2O:pyrimidine = 20:1 mixture, several mixtures with the same composition were photo-irradiated to confirm these results.

Finally, two additional irradiation experiments were performed starting from a H_2O:pyrimidine = 20:1 ice mixture:

one under similar conditions to those described above but with a temperature of 120 K to simulate conditions more relevant to Solar System icy environments, and one with a CaF_2 window used to filter out Lyman α photons emitted by the UV lamp and measure the effect of the UV irradiation wavelength. Both of these samples were analyzed with high-performance liquid chromatography and gas chromatography–mass spectrometry techniques.

2.2. Infrared spectroscopy at low temperature

To verify the ratios between H_2O and pyrimidine in the mixtures and monitor the evolution of the ices upon UV photo-irradiation, an H_2O:pyrimidine ice mixture was deposited at 14 K onto an IR-transparent ZnSe window for 2 min at a rate of $\sim 0.20\ \mu m\ min^{-1}$. This window is mounted in a vacuum chamber placed in a Bio-Rad Excalibur Series Fourier-transform infrared spectrometer equipped with a mercury-cadmium-telluride detector cooled to 77 K with liquid nitrogen. The ice mixture was photo-irradiated with a similar H_2 UV lamp at 14 K at increasing intervals of 15, 30, 60, 120, and 180 min. The evolution of the mixture during the irradiation increments and heating to room temperature was monitored by IR spectroscopy. Sample spectra (resolution: $1\ cm^{-1}$) were obtained by averaging 1000 scans and then dividing by a spectrum of the chamber and blank cold sample window taken before deposition. Photodestruction of pyrimidine was monitored via its strongest IR bands at $\sim 1587\ cm^{-1}$ (ν_{CN}, ν_{CC}) and $\sim 1406\ cm^{-1}$ (β_{CH}, ν_{CN}) (see Destexhe *et al.*, 1994, and Fig. 3b). Abundances were determined from the initial (pre-irradiated) spectrum of the H_2O: pyrimidine mixture.

2.3. High-performance liquid chromatography analysis of the residues at room temperature

Samples dissolved in H_2O were injected into a Hewlett Packard/Agilent 1100 Series high-performance liquid chromatograph (HPLC) device equipped with a Phenomenex Luna 5μ Phenyl-Hexyl column (size: 250×4.60 mm; inner diameter: 5 μm). The volume of solution injected for each independent run was 5 μL. The eluting compounds were detected by a diode-array UV detector (Agilent G1315A), which recorded the signals at 220, 245, 256, 280, and 300 nm, and a fluorescence detector (Agilent G1321A) with excitation and emission wavelengths of 250 and 450 nm, respectively.

The method used a total run time of 60 min and the following solvent gradients: 0–15 min, 100% ammonium formate buffer (pH = 5); 15–22 min, ramping to 12% CH_3OH, 5% buffer, 83% H_2O; 22–60 min, ramping to 20% CH_3OH, 5% buffer, 75% H_2O, at a constant flow of $0.5\ mL\ min^{-1}$. The 50 m*M* ammonium formate buffer was prepared in our laboratory from H_2O (18.2 MΩ cm resistivity, Millipore Direct-Q UV 3), CH_3OH (Aldrich, Chromasolv®, ≥99.9% purity), formic acid HCOOH (Sigma-Aldrich, reagent grade, ≥95% purity), and ammonium hydroxide NH_4OH (Sigma-Aldrich, 4.98 *N* solution in water). The pH of the buffer was adjusted by addition of NH_4OH until a pH of 5 was obtained.

The identification of the peaks on the HPLC chromatograms was performed by comparing their retention times and UV spectra with those of standards dissolved to $10^{-3}\ M$ in H_2O and injected into the HPLC device by using the same method as for the samples. The standards used in this study include pyrimidine itself (Aldrich, 99% purity) and a variety of singly, doubly, and triply oxidized pyrimidine derivatives: 2-hydroxypyrimidine (hydrochloride; Aldrich, 98% purity), 4(3*H*)-pyrimidone (Aldrich, ≥98% purity), uracil (Aldrich, 98% purity), 4,6-dihydroxypyrimidine (Aldrich, 98% purity), barbituric acid (Fluka, ≥99% purity), and isobarbituric acid (Aldrich, approximately 98% purity). In addition, we searched for a few other pyrimidine derivatives: 2,2′-bipyrimidine (Aldrich, 97% purity), 1,4,5,6-tetrahydropyrimidine (Aldrich, 97% purity), 2-pyrimidinecarbonitrile (Aldrich, 97% purity), and orotic acid (monohydrate; Sigma, 97% purity). The molecular structures of all these compounds are shown in Figs. 1 and 2.

Samples and standards were also dissolved in 500 μL of CH_3OH (Aldrich, Chromasolv®, ≥99.9% purity) instead of H_2O to compare the effect of the solvent. When CH_3OH was used as the solvent, the peaks in the chromatograms became broader and overlapped more with each other, which rendered the peak identification more difficult. For this reason, H_2O was used as a solvent for all the samples presented in this work.

2.4. Gas chromatography–mass spectrometry analysis of the residues at room temperature

The foils that contained the residues for gas chromatography–mass spectrometry analysis were shaken with 100 μL of ethyl acetate ($CH_3COOCH_2CH_3$, Fisher Scientific, Optima

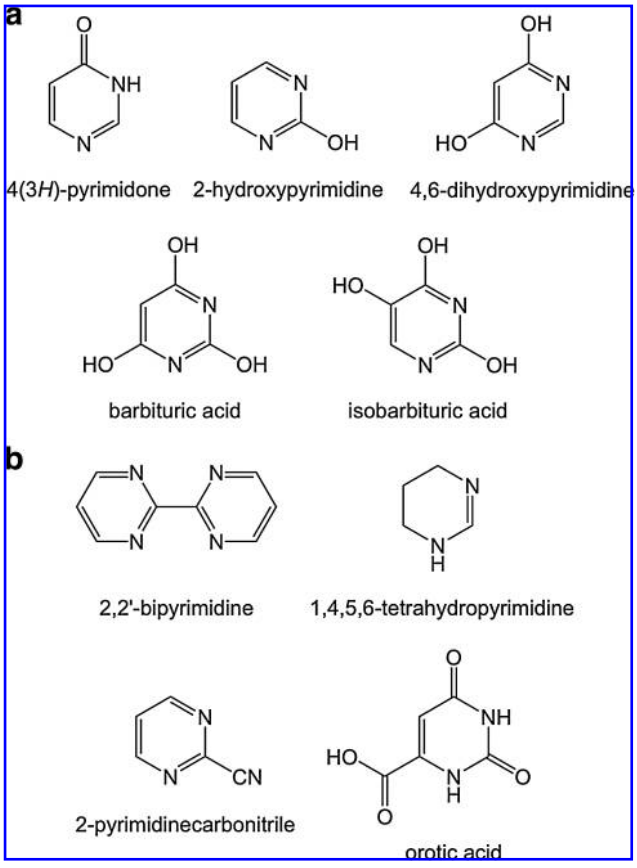

FIG. 2. Molecular structures of (**a**) singly, doubly, and triply oxidized pyrimidine derivatives, and (**b**) additional pyrimidine derivatives searched for in this work.

grade). The ethyl acetate extracts were then transferred to a clean vial that had previously been pyrolyzed overnight in a muffle furnace at 550°C. We then added 20 μL of a mixture of *N*-methyl-*N*-(*tert*-butyl-dimethylsilyl)-trifluoroacetamide (Sigma-Aldrich, >97% purity), dimethylformamide (Pierce, silylation-grade solvent), and pyrene (Sigma-Aldrich, analytical standard, 100 ng μL^{-1} dissolved in cyclohexane) in relative proportions 3:1:1 to the dried residues and heated at 100°C for 1 h to convert N–H and O–H bonds into their *tert*-butyldimethylsilyl derivatives (MacKenzie *et al.,* 1987; Casal *et al.,* 2004).

Separation was carried out with a Thermo Trace gas chromatograph coupled to a DSQ mass spectrometer with a splitless injection, an injector temperature of 250°C, and a flow of 1.3 mL min^{-1}. A Restek Rxi®-5ms column was used (length: 30 m, inner diameter: 0.25 mm, film thickness: 0.50 μm). Temperature was held at 100°C for 1 min, then ramped at 5°C min^{-1} to 250°C, then held for 5 min. Masses were recorded from 50 to 550 atomic mass units (amu), and data analysis was performed with Xcalibur™ software (Thermo Finnigan).

3. Results

3.1. Infrared spectroscopy

In the experiment in which we monitored the behavior upon UV photo-irradiation of an H_2O:pyrimidine = 20:1 ice mixture with IR spectroscopy, abundances were determined from the initial (pre-irradiated) spectrum of the ice mixture by using its strong IR bands at ~1587 cm^{-1} and ~1406 cm^{-1} (see Section 2.2 and Fig. 3b). These two bands are analogous to those for pyrimidine in the gas phase or isolated in cold argon (Ar) matrix both in positions and relative intensities (Destexhe *et al.,* 1994) and are similar to the bands of pure pyrimidine vapor deposited on the same substrate under comparable experimental conditions in our vacuum system. The column density of H_2O was determined to be $N = 1.1\times10^{18}$ molecule cm^{-2} derived from the integrated area (in absorbance), accurate to 5%, of the main feature at 3298 cm^{-1}, with an integrated absorbance (A) value of 1.7×10^{-16} cm $molecule^{-1}$ (Hudgins *et al.,* 1993).

Assuming an H_2O:pyrimidine ratio of 20:1, the A values for the 1587 and 1406 cm^{-1} bands for pyrimidine are then $8.1\pm0.7\times10^{-18}$ cm $molecule^{-1}$ and $6.7\pm0.9\times10^{-18}$ cm $molecule^{-1}$, respectively. Figure 3 shows the spectrum of the freshly deposited ice, the spectrum of the same ice after 180 minutes of vacuum UV irradiation, and several spectra taken during warm-up to 250 K. Comparing the spectrum of the unirradiated ice with that taken after irradiation shows that the strong pyrimidine bands are reduced by about 70%, while new features grow at 2342, 2252, 2167, 2138, and 2090 cm^{-1}. Most of the new bands were distinguishable after 30 min of UV irradiation and became more evident with further exposure. The three bands at 2342, 2167, and 2138 cm^{-1} are readily assigned to CO_2, OCN^-, and CO (*e.g.,* Sandford *et al.,* 1988; Sandford and Allamandola, 1990; Schutte and Greenberg, 1997; Demyk *et al.,* 1998). The band at 2252 cm^{-1} falls in the nitrile (C≡N) stretching region (Bernstein *et al.,* 1997), but the carrier has not been identified. A similar situation holds for the 2090 cm^{-1} band, which falls in the isonitrile region (Silverstein and Bassler, 1967; Bernstein *et al.,* 1997). The growth of the CO_2 peak is correlated with the destruction of pyrimidine, which suggests that a free source of carbon is derived as one or more of the photoproducts of pyrimidine.

Based on these A values determined for the 1587 and 1406 cm^{-1} pyrimidine bands, a column density was derived for each irradiation interval, with an accuracy of ~5%. By monitoring this column density during the photolysis, an estimate of the half-life can be derived for an optically thin ice from a first-order decay (Cottin *et al.,* 2003):

$$N(t) = N_0 \exp(-Jt) \quad (1)$$

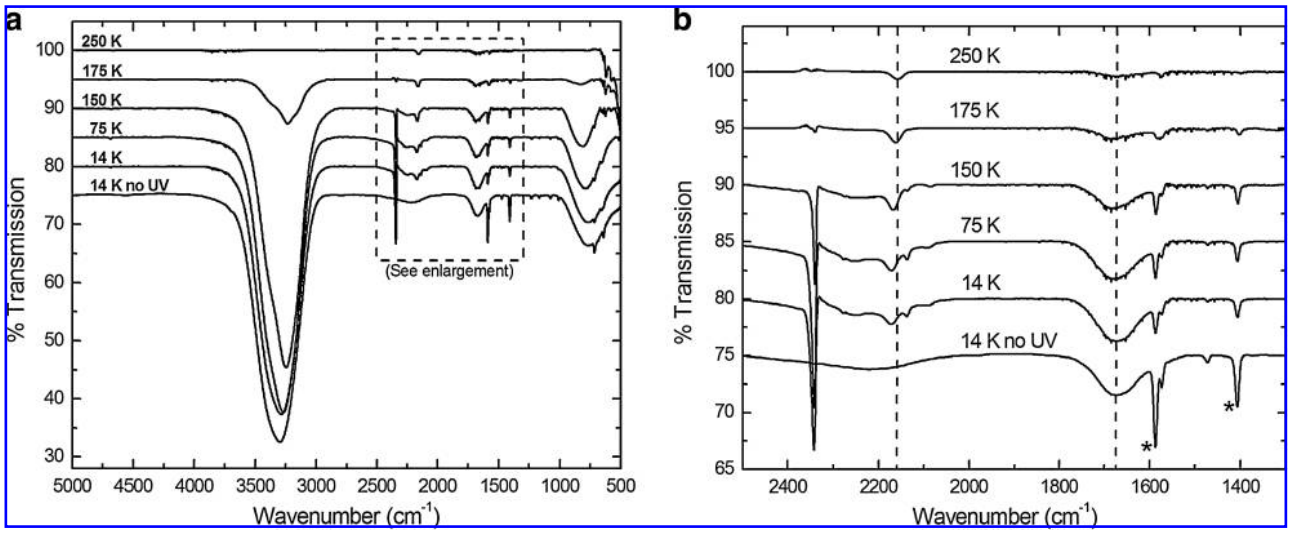

FIG. 3. (**a**) Infrared spectra of a H_2O:pyrimidine = 20:1 mixture deposited at 14 K before UV photo-irradiation and after a 180 min irradiation with the H_2 UV lamp during warm up at 14, 75, 150, 175, and 250 K. (**b**) Enlargement showing the IR bands at ~2152 and ~1665 cm^{-1} (dashed lines), which remain during the warm-up. The two IR bands at 1587 and 1406 cm^{-1}, marked with an asterisk (*) were used to estimate the column densities of pyrimidine in the sample. The photolytic half-life of pyrimidine was derived from the decay of the 1406 cm^{-1} band.

where J is the product of the UV destruction cross section of the molecule σ (cm^2 $molecule^{-1}$), and the UV flux I (photons cm^{-2} s^{-1}). The cross sections obtained for pyrimidine in H_2O ice were $\sigma = 1.5\times10^{-19}$ cm^2 $molecule^{-1}$ for both the 1587 and 1406 cm^{-1} bands, given with an accuracy within 5%, obtained from least-square exponential fits for each band (R^2 values: 0.9553 and 0.9927 for the 1587 and 1406 cm^{-1} bands, respectively). From these values, half-lives for the laboratory, diffuse ISM, dense clouds, and the Solar System (at ~1 AU) could be directly determined by using appropriate UV fluxes of 2×10^{15} photons cm^{-2} s^{-1} (Bernstein *et al.*, 1999; Elsila *et al.*, 2007), 8×10^{7} photons cm^{-2} s^{-1} (Mathis *et al.*, 1983), 1×10^{3} photons cm^{-2} s^{-1} (Prasad and Tarafdar, 1983), and 3×10^{13} photons cm^{-2} s^{-1} (Peeters *et al.*, 2005), respectively. The half-lives derived from the 1406 cm^{-1} band data are listed in Table 1 and compared to those measured by Peeters *et al.* (2005) for pyrimidine in an Ar matrix. The half-life of pyrimidine in pure H_2O ice (this work) was found to be up to ~2 orders of magnitude longer than in argon. Therefore, when embedded in pure H_2O ice, pyrimidine could survive about 1.43×10^{8} years under conditions typical of dense parts of interstellar clouds. In the Solar System, the half-life of pyrimidine at the UV-exposed surface of icy bodies, such as comets and icy satellites, is estimated to be only 42 h. However, if pyrimidine is incorporated deeper than the penetration depth of UV photons in the ice of comets and asteroids, its lifetime may be long enough to survive until it is delivered to Earth and other telluric planets.

The spectrum of the irradiated ice was also monitored at specific temperatures as it was warmed to room temperature to study the stability of the newly formed species in the samples. Figure 3 shows that the bands from unreacted pyrimidine remain fairly constant up to about 150 K, the temperature at which the H_2O ice begins to rapidly sublime. The pyrimidine loss above 150 K seems to track with H_2O loss, behavior which appears to hold for most of the new bands produced by photo-irradiation.

The 2167 cm^{-1} (OCN^-) band is the exception. This feature remains evident to temperatures around 250 K, though it appears slightly blue-shifted as the temperature increases (see Fig. 3b). This behavior is consistent with earlier studies of this feature, formerly referred to as XCN (Lacy *et al.*, 1984; Allamandola *et al.*, 1988; Bernstein *et al.*, 1995; Palumbo *et al.*, 2000). In view of the production of the OCN^- feature and of the nitriles and isonitriles, suggested by the 2252 and 2090 cm^{-1} bands, we searched for the presence of nitrile derivatives of pyrimidine in the residues (see Sections 2.3 and 3.2).

As H_2O is depleted, evidence of multiple bands remaining near 1665 cm^{-1} suggests a source other than H_2O (Fig. 3b). These features can be attributed to the C=C and C=O stretching modes found for pyrimidine in H_2O solvent studies (Gaigeot and Sprik, 2003). Finally, there are some minor bands in the ~3000–2800 cm^{-1} CH_3/CH_2 stretching region, which implies some ring structures were broken, or pyrimidine molecules were hydrogenated during the irradiation and warm-up. This is further supported by subtle features near 1465 cm^{-1}, corresponding to the CH_2 deformation modes. We searched for hydrogenated pyrimidine derivatives in the residues by using high-performance liquid chromatography but were unable to verify their presence (see Sections 2.3 and 3.2).

3.2. Liquid chromatography

The total HPLC chromatogram for the $\lambda = 256$ nm signal of a residue produced from a typical H_2O:pyrimidine = 20:1 mixture irradiated with UV photons at 26–31 K for ~23 h is shown in the top trace of Fig. 4a. The bottom trace, which corresponds to a control sample where only pure H_2O ice was deposited and UV-irradiated during the same time, clearly shows that no contaminants were present. Two additional control experiments were also run. In the first one, a similar H_2O:pyrimidine = 20:1 mixture was deposited but not exposed to UV. In the second one, no ice was deposited onto the foil during the normal UV irradiation time. These two samples verified that the complexity of the irradiated sample is not due to contamination or reactions of the gas mixture before deposition. Chromatograms obtained from the residues dissolved in H_2O on the first day and up to 25 days later show no significant differences, indicating that the compounds constituting the residues are stable with time and hydrolysis.

Only 4(3*H*)-pyrimidone, a singly oxidized derivative of pyrimidine (Fig. 2a), was conclusively identified as an oxidized pyrimidine product from high-performance liquid chromatography. Its identification was confirmed through a match of both the retention time (8.77 min) and UV spectrum of the standard (Figs. 4b and 5b, respectively). The peak associated with 4(3*H*)-pyrimidone, labeled as peak **1** in all chromatograms, is one of the most intense of all our H_2O:pyrimidine samples.

Uracil was tentatively identified in our samples with high-performance liquid chromatography by the retention time and UV spectrum of the peak eluting at 8.51 min in the

Table 1. Comparison between the UV-Destruction Cross Sections (σ_{UV}) and Half-Lives of Pyrimidine Mixed with H_2O Ice (This Work) and Isolated in an Ar Matrix (Peeters *et al.*, 2005)

		Half-lives[a]			
Mixture	σ_{UV} (cm^2 $molecule^{-1}$)	*Laboratory (min)*	*DISM*[b] *(yr)*	*DC*[b] *(Myr)*	*Solar System (hr)*
Pyrimidine:H_2O (1:20)[c]	1.5×10^{-19}	38	1430	143	42
Pyrimidine:Ar (1:750)[d]	2.7×10^{-17}	0.93	8.1	0.81	0.23

[a]Estimated according to the UV photon fluxes from the literature (see Section 3.1).
[b]DISM and DC stand for diffuse interstellar medium and dense clouds, respectively.
[c]Data derived from the 1406 cm^{-1} band.
[d]Data from Peeters *et al.* (2005).
Myr, millions of years.

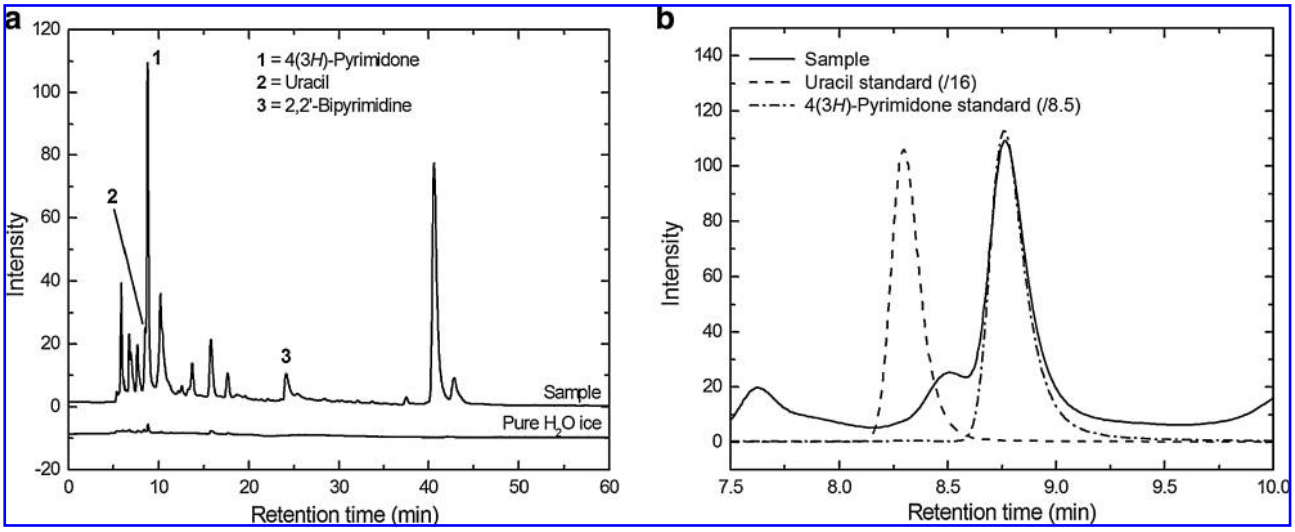

FIG. 4. (**a**) Total HPLC chromatograms (256 nm signal) of the sample prepared from the UV photo-irradiation of a H_2O:pyrimidine = 20:1 mixture at 26–31 K over 23 h (top trace) and of a blank experiment where only pure H_2O ice was deposited and UV irradiated for the same time duration (bottom trace, offset for clarity). The identified compounds are indicated by peaks marked with numbers. (**b**) Enlargement of the sample chromatogram around the retention times at which uracil and 4(3*H*)-pyrimidone elute (solid trace). The chromatograms of the uracil (dashed trace) and the 4(3*H*)-pyrimidone (dot-dashed trace) standards are given for a direct comparison. The assignment of the peak at 8.51 min to uracil is supported by its UV spectrum (see Fig. 5a).

sample chromatogram (Fig. 4b, solid trace). However, this peak, labeled **2** in the chromatograms, is blended with that of 4(3*H*)-pyrimidone, which has the effect of shifting the peak center and renders the comparison of the retention times between the sample and the uracil standard more difficult. However, as shown in Fig. 5a, the main absorption band in the UV spectrum of this peak matches very well with the main absorption band measured for the uracil standard.

Among the non-oxidized pyrimidine derivatives (Fig. 2b), only 2,2′-bipyrimidine could be identified in the HPLC chromatograms of the residues (Fig. 4a, top trace), from both its retention time of 24.16 min and UV spectrum, which displays a large band centered at 240 nm. Its peak is labeled **3** in all the chromatograms. The presence of this compound, comprised of two molecules of pyrimidine linked together by a C–C bond between the carbon atoms in positions 2 (*i.e.*, the carbon atom between the two nitrogen atoms in the molecular structure, see Fig. 2b), shows that one of the effects of the UV photons on pyrimidine is to activate or ionize particular atoms lacking electronic density, so that they can chemically react with other nearby species, including other pyrimidine molecules. Other structures of bipyrimidines are also possi-

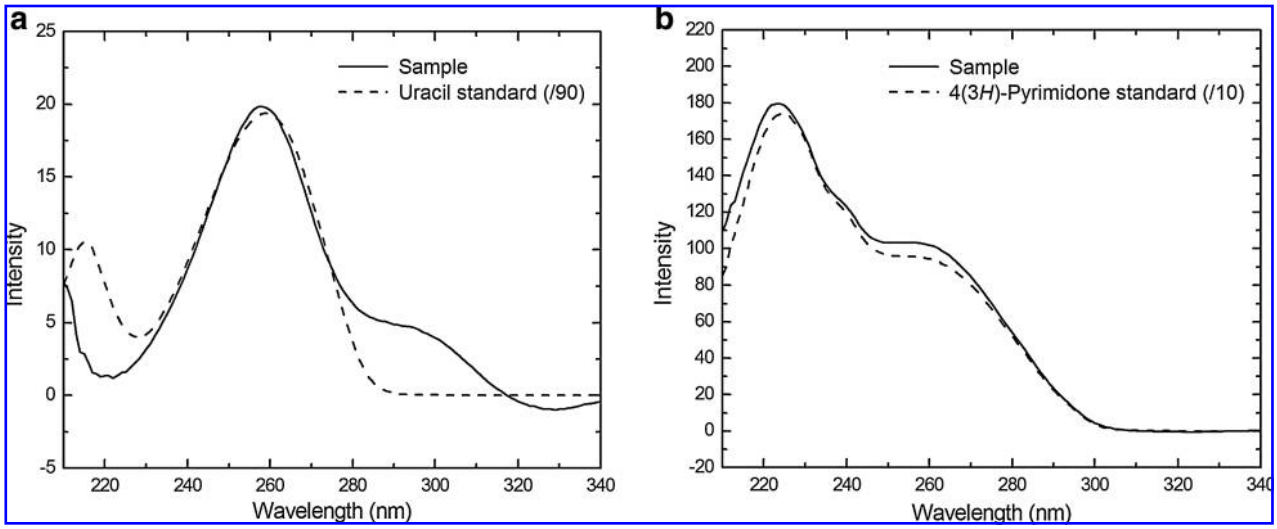

FIG. 5. (**a**) UV spectra of the sample peak eluting at 8.51 min and assigned to uracil (solid trace), and a uracil standard (10^{-3} *M* in H_2O, dashed trace). (**b**) UV spectra of the sample peak eluting at 8.77 min and assigned to 4(3*H*)-pyrimidone (solid trace), and a 4(3*H*)-pyrimidone standard (10^{-3} *M* in H_2O, dashed trace). These UV spectra correspond to the peaks on the sample chromatogram obtained for the H_2O:pyrimidine = 20:1 mixture shown in Fig. 4.

ble, but their standards are not commercially available; thus we could not search for them in our samples. Although we also performed a control experiment in which pure pyrimidine ice (no H_2O) was photo-irradiated, we were unable to determine whether 2,2′-bipyrimidine was formed under these conditions because of the broad coeluting peak of unreacted pyrimidine that obscures any potential 2,2′-bipyrimidine peak.

The remaining peaks seen in the chromatograms of the residue (Fig. 4a, top trace), and of all other residues produced from the UV photo-irradiation of H_2O:pyrimidine mixtures, remain unidentified because neither their retention times nor their UV spectra correspond to any of the other available standards listed in Section 2 and illustrated in Fig. 2. These unidentified peaks could be due either to pyrimidine derivatives for which we do not have the standards or to products stemming from the photofragmentation of pyrimidine, as suggested by the IR spectroscopy results (Section 3.1).

It is particularly interesting to note that no 1,4,5,6-tetrahydropyrimidine was found, indicating that high-degree hydrogenation of pyrimidine in H_2O ice subjected to UV photons is not as efficient as observed for small PAHs (Bernstein *et al.*, 1999, 2001, 2002b; Ashbourn *et al.*, 2007) and PANHs (Elsila *et al.*, 2006) mixed in pure H_2O ices. Less-hydrogenated compounds may be present in our samples and could account for some of the unidentified peaks, but a search for such compounds would have been very difficult since suitable standards were not available. Hydrogenated pyrimidines may thus account for only a small fraction of the bands assigned to CH_3 and CH_2 groups in the IR spectra of the residues (see Section 3.1 and Fig. 3).

According to the IR spectra, some of the unidentified peaks might be assigned to compounds that contain either nitrile ($-C\equiv N$)/isonitrile ($-N\equiv C$) or carboxylic acid (COOH)/carboxylate (COO^-) groups, or both. However, neither of the two standards bearing a nitrile or a carboxylic acid group, namely, 2-pyrimidinecarbonitrile and orotic acid (Fig. 2b), respectively, were found in our residues. Peaks displaying a mass spectrum with an intense peak at 181 amu, which could correspond to the mass expected for pyrimidic acids, have been identified in the gas chromatograph–mass spectrometer (GC-MS) chromatograms at 14.09 and 16.88 min, but the lack of standards cannot confirm their presence in our samples.

Among the unidentified peaks in the chromatograms, two peaks eluting at 40.60 and 42.82 min are of particular interest. These peaks appear in the chromatograms of all the samples prepared from the UV irradiation of H_2O:pyrimidine mixtures with the intensity of the first peak comparable to, or higher than, those for the peaks of other photoproducts, including 4(3*H*)-pyrimidone. Moreover, they elute at much longer times than all other peaks suspected to be due to oxidized pyrimidine photoproducts. The UV spectra of these two peaks are similar to each other, having two main absorption bands around 233 and 265 nm, and are distinguishable from the UV spectra of other peaks in the chromatograms of the samples and standards. This holds true for samples with different starting ratios of H_2O and pyrimidine and for pure pyrimidine ice. These results suggest that these peaks probably correspond to stable photoproducts of pyrimidine, which may either be noncyclic compounds formed from the photodestruction of pyrimidine, other cyclic compounds (*e.g.*, 5-atom rings), or higher-degree pyrimidine oligomers (more than two molecules).

Experiments with initial relative proportions between H_2O and pyrimidine of 10:1, 40:1, and 100:1 were also performed at 20–30 K. The chromatograms obtained for these residues are very similar to each other and are comparable to the chromatogram of the residue produced from the H_2O:pyrimidine = 20:1 starting mixture shown in Fig. 4a. Comparison of all these chromatograms suggests that the relative proportion between H_2O and pyrimidine in the starting mixture in the 10–100 range does not significantly affect the chemistry. This clearly indicates that H_2O is not a limiting reactant in these processes and can be photodestroyed by the UV photons regardless of the relative amount of pyrimidine in the ice. Also, only very small amounts, if any, of unreacted pyrimidine were detected in the chromatograms, which shows that our H_2O ices were transparent for UV photons to irradiate the entire ice.

The chromatograms of the residues produced from the UV irradiation of a H_2O:pyrimidine = 20:1 mixture at 120 K instead of 20–30 K, and from the UV irradiation with the use of CaF_2 filter to cut off photons with wavelengths shorter than 130 nm including Lyman α (121.6 nm), are shown in Fig. 6a and 6b, respectively. Both chromatograms are strikingly similar, and both resemble the residue produced at 20–30 K without the CaF_2 filter (Fig. 4a). The relative intensities between the peaks vary slightly, but the same peaks are present in all three chromatograms (Figs. 4a, 6a, and 6b). Another similarity is the presence of the two peaks eluting in the 40–45 min range, as observed in all other chromatograms of residues discussed.

3.3. Gas chromatography/mass spectrometry

The gas chromatography–mass spectrometry analysis of the extracted residue from a H_2O:pyrimidine = 20:1 photo-irradiated ice also revealed the presence of multiple compounds not present in the non-irradiated ice control, as shown in their total-ion chromatograms (top and bottom traces of Fig. 7, respectively). The product suite includes a number of peaks with masses that correspond to singly and doubly oxidized pyrimidines. Figure 8 shows two chromatograms of the same residue in the single-ion mass mode of the GC-MS device for the selected masses of mass-to-unit charge ratio $m/z = 153$ (top trace) and 283 amu (middle trace), corresponding to the masses of the singly and doubly oxidized pyrimidine derivatives, respectively. Uracil (peak **2**, eluting at 20.19 min) was conclusively identified in this residue by comparison of the $m/z = 283$ amu single-ion chromatograms (doubly oxidized pyrimidines) of the sample (middle trace) and that of the standard (bottom trace, Fig. 8). This definitely confirms the results obtained from high-performance liquid chromatography analysis on the presence of uracil in the residues.

Among the singly oxidized compounds ($m/z = 153$ amu, top trace), 4(3*H*)-pyrimidone has been identified with gas chromatography–mass spectrometry, although it does not appear on Fig. 8 because it elutes at a shorter retention time, confirming its detection with high-performance liquid chromatography (Section 3.2). Other singly and doubly oxidized ($m/z = 283$ amu, middle trace) pyrimidine derivatives may be present in the samples, as suggested by the other peaks on

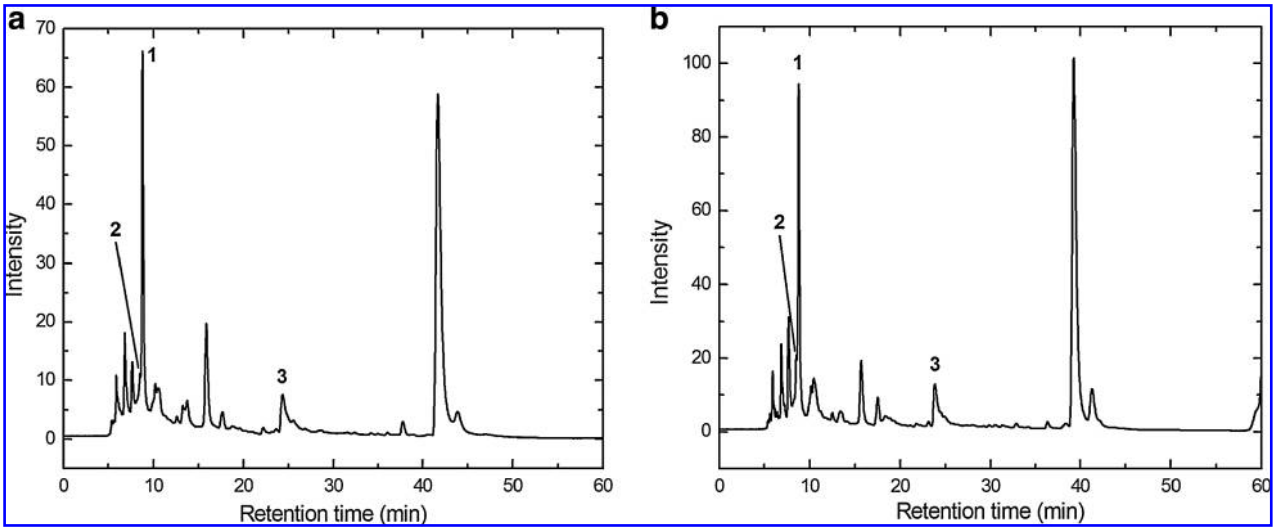

FIG. 6. HPLC chromatograms (256 nm signals) of (**a**) a sample prepared from the UV photo-irradiation of a H_2O:pyrimidine = 20:1 mixture at 120 K and (**b**) a sample prepared from the UV photo-irradiation of a H_2O:pyrimidine = 20:1 mixture when a CaF_2 filter was used to cut off photons with wavelengths shorter than 130 nm, including the Lyman α transition (121.6 nm). In both chromatograms, the peaks marked with numbers refer to the identified compounds (see Fig. 4a).

Fig. 8. However, no 2-hydroxypyrimidine (shorter retention time) and no 4,6-dihydroxypyrimidine (retention time of the standard: 21.00 min) were detected in this residue. The presence of 2,2′-bipyrimidine could also be confirmed by gas chromatography–mass spectrometry analysis via its peak at 17.19 min and its mass spectrum displaying a main peak at $m/z = 158$ amu, which corresponds to the total-ion mass for this compound, as well as probably other bipyrimidine isomers, eluting at 12.53 and 16.27 min, whose peaks have very similar mass spectra with a main mass peak at 158 amu.

Finally, two samples—one H_2O:pyrimidine = 20:1 ice mixture photo-irradiated at 120 K and another one at 20–30 K with use of a CaF_2 filter—were analyzed by gas chromatography–mass spectrometry, and the obtained chromatograms were compared with the high-performance liquid chromatography analyses. The total-ion chromatograms for these two residues

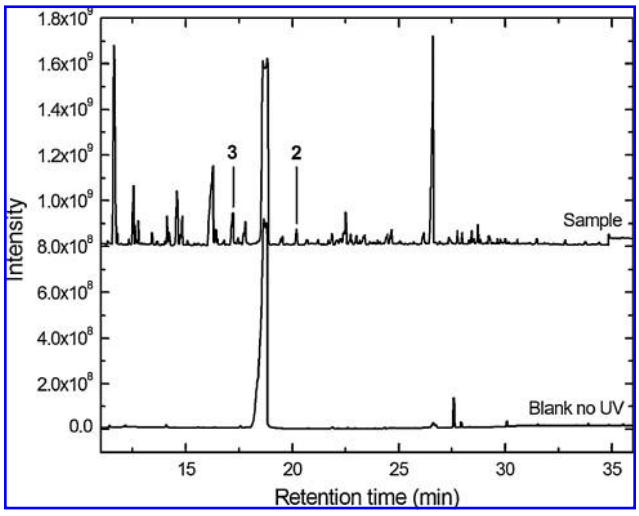

FIG. 7. Total-ion GC-MS chromatogram of a residue prepared from a H_2O:pyrimidine = 20:1 mixture either exposed to UV irradiation under the same conditions as for the residues analyzed by HPLC (top trace, offset for clarity) or not exposed to UV irradiation (bottom trace). The peak labeled **2** eluting at 20.19 min corresponds to uracil (see Figs. 4a and 8). The intense peak eluting at ~18.7 min in both traces is due to a derivatization by-product, while the peak at ~27 min represents pyrene, used as an internal standard.

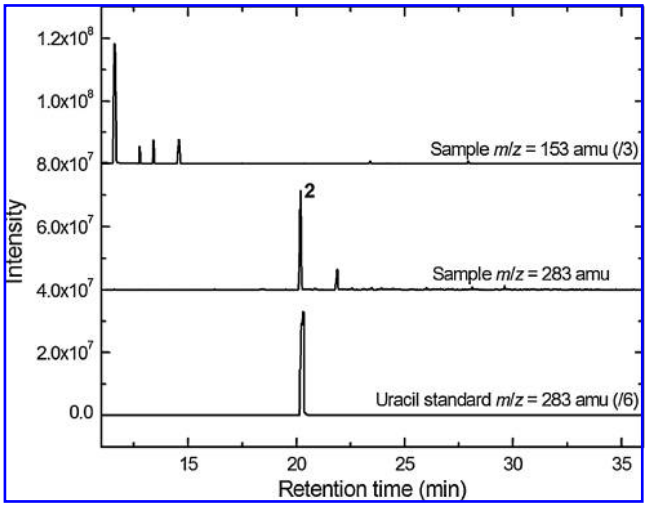

FIG. 8. Single-ion GC-MS chromatograms for a residue prepared from the UV photo-irradiation of a H_2O:pyrimidine = 20:1 mixture: single-ion chromatogram for $m/z = 153$ amu (corresponding to singly oxidized pyrimidines, top trace, offset for clarity) and single-ion chromatogram for $m/z = 283$ amu (doubly oxidized pyrimidines, middle trace, offset for clarity). The peak labeled **2** eluting at 20.19 min (middle trace) was identified as uracil by comparison with a single-ion chromatogram injection for $m/z = 283$ amu of a uracil standard (bottom trace).

are shown in Fig. 9a and 9b, respectively. Whereas the high-performance liquid chromatography analyses did not show any clear difference between these samples (Fig. 6), the GC-MS chromatograms show some differences. In particular, the chromatogram of the residue where the CaF_2 filter was used shows a smaller number of peaks (Fig. 9b) than both the chromatograms obtained for samples prepared without the filter at 120 K (Fig. 9a) and at 20–30 K (Fig. 7, top trace). This suggests that, in ices where short-wavelength UV photons (Lyman α) cannot penetrate, the (photo)chemistry is less efficient and less complex. The reason why this difference does not appear in the HPLC chromatograms (Figs. 4a and 6) is not clear, but it may be due to effects from the analytical methods themselves, as some photoproducts are more easily seen in the GC-MS chromatograms than in the HPLC chromatograms (*e.g.*, uracil).

4. Discussion

4.1. Temperature and UV wavelength dependence for the formation of oxidized photoproducts

The UV photo-irradiation of H_2O:pyrimidine mixtures at low temperature leads to the formation of organic residues that contain a multitude of compounds of which 4(3*H*)-pyrimidone and uracil are the major identified oxidized photoproducts. The global behavior is similar to the UV photo-irradiation of PAHs in H_2O, where the primary effect of the UV photons is to break H_2O molecules, as well as to modify the pyrimidine molecules by ionizing them, removing peripheral atoms, fragmenting them, or any combination of these processes. These processes yield highly reactive pyrimidine and H_2O photoproducts within the ice that can either react immediately with neighboring molecules or react as the ice is further warmed and its constituents become more mobile. The formation of these reactive photoproducts is similar to that previously observed for the alteration of PAHs (Bernstein *et al.*, 1999, 2001, 2002b; Ashbourn *et al.*, 2007) and PANHs (Elsila *et al.*, 2006) in ices, as well as for the formation of amino acids in irradiated ices (Bernstein *et al.*, 2002a; Muñoz Caro and Schutte, 2003; Nuevo *et al.*, 2008), and is largely independent of the initial ice temperature. In all cases, the formation of oxidized pyrimidines most likely takes place when reactive radicals and ions react with neighboring species in the ice matrix during the warm-up.

In addition, the chromatograms shown in Figures 6b (HPLC) and 9b (GC-MS), which were obtained for residues formed with the use of a CaF_2 filter, suggest that the photon energy is not a critical parameter in these experiments, since in all cases photoproducts were formed with similar distribution and absolute abundances as is indicated in the chromatograms obtained for residues formed without the use of the filter (Figs. 4a and 7 for HPLC and GC-MS, respectively). The GC-MS data, however, show that there are some differences. We anticipate that similar chemistry would be seen for H_2O:pyrimidine ices irradiated with energetic protons, since it has been shown that the residues formed from the UV photo-irradiation and the 1 MeV proton bombardment of interstellar ice analogues display similar infrared spectra (Gerakines *et al.*, 2001), and both UV and proton irradiations on PAHs yield essentially the same products (Bernstein *et al.*, 2002b, 2003).

4.2. Formation of uracil: reaction yield and pathways

During the experiment that led to the formation of the organic residue whose HPLC chromatogram is given in Fig. 4, the total amount of H_2O:pyrimidine = 20:1 ice mixture that was deposited on the Al foil and photo-irradiated was 2.94 ± 0.01 mmol (2.80 ± 0.01 mmol of H_2O and 0.14 ± 0.01 mmol of pyrimidine).

To estimate the quantities of 4(3*H*)-pyrimidone and uracil formed in our samples, we prepared and injected three 4(3*H*)-pyrimidone:uracil mixtures with relative proportions 1:1, 5:1, and 10:1. From the HPLC chromatograms obtained, we could establish a linear correlation between the relative

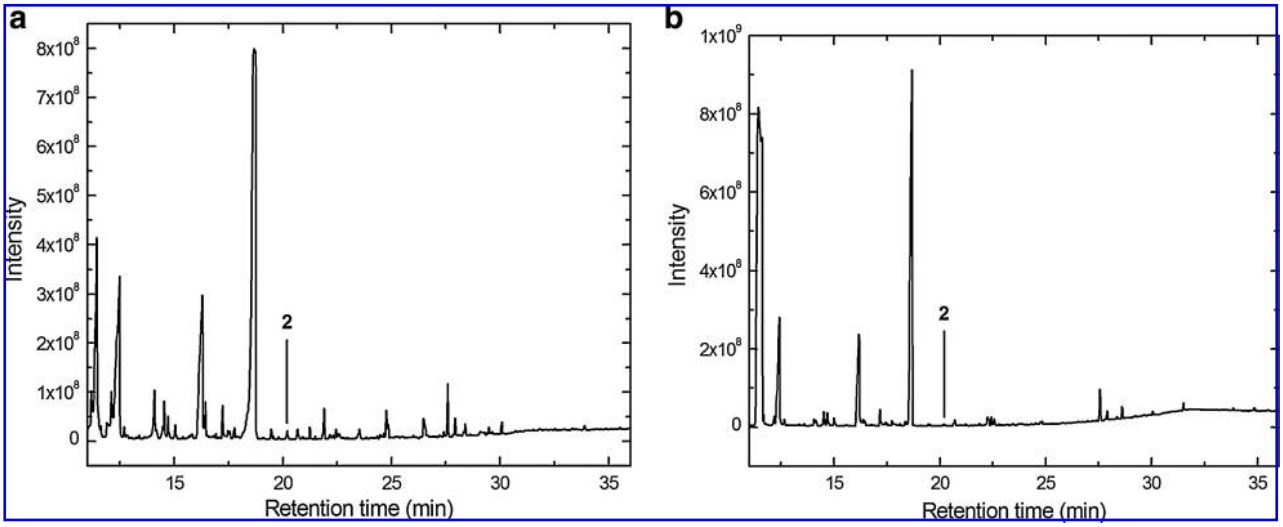

FIG. 9. Total-ion GC-MS chromatograms of (**a**) the sample prepared from the UV photo-irradiation of a H_2O:pyrimidine = 20:1 mixture at 120 K and (**b**) the sample prepared from the UV photo-irradiation of a H_2O:pyrimidine = 20:1 mixture with a CaF_2 filter (see also Fig. 6). In both chromatograms, the peaks labeled **2** refer to uracil (see Fig. 4a).

proportions of these two standards and the areas of their peaks ($R^2 = 0.99993$). We then measured the peak areas of 4(3*H*)-pyrimidone and uracil in the chromatogram of the sample (Fig. 4b, solid trace) and deduced that in this sample the 4(3*H*)-pyrimidone is 10.9 ± 0.4 times more abundant than uracil. From the chromatogram of the 4(3*H*)-pyrimidone standard (Fig. 4b, dot-dashed trace) and its known concentration (10^{-3} *M* in H_2O), we estimated the quantity of this compound to be ~ 5 nmol in the 5 μL of standard injected in the HPLC column. By comparison between the areas of the peaks in this standard injection and the sample chromatogram, and assuming that the 5 μL of sample injected in the column is representative of the whole extract (*i.e.*, 500 μL), we estimate the quantities of 4(3*H*)-pyrimidone and uracil formed in our sample to be 59.1 ± 2.3 nmol and 5.4 ± 0.2 nmol, respectively. Therefore, the molecular yields relative to pyrimidine, that is, the fractions of 4(3*H*)-pyrimidone and uracil in our sample formed from the UV photo-irradiation of the initial pyrimidine, are 4.2×10^{-4} and 4×10^{-5}, respectively. In other words, under our experimental conditions, of $\sim 2.5 \times 10^4$ molecules of pyrimidine photo-irradiated in the presence of H_2O ice, 10 will be converted into 4(3*H*)-pyrimidone, and one will be converted into uracil.

The mechanisms of formation of these oxidized derivatives of pyrimidine are not currently well understood, though some patterns can be seen in our experiments (Fig. 10). The fact that 4(3*H*)-pyrimidone was found to be the most abundant oxidized pyrimidine derivative in our samples and 2-hydroxypyrimidine was not detected in any of them indicates a chemical regioselectivity for the addition of the first oxygen atom to pyrimidine. Thus, the position labeled 4 in the pyrimidine molecule in Fig. 10, that is, the two equivalent carbon atoms bound to one nitrogen atom and another carbon atom in the ring structure, seems to be favored. Consequently, the first oxidized pyrimidine derivative formed is most likely 4(3*H*)-pyrimidone; then the second oxygen atom to form uracil is added in position 2 only after the first oxygen atom has been added in position 4. This mechanism implies that uracil may be a (photo)product of 4(3*H*)-pyrimidone. In this case, the molecular yield for the formation of uracil from 4(3*H*)-pyrimidone would be $\sim 8\%$ under our experimental conditions. At the same time, 4(3*H*)-pyrimidone could as well be converted into other doubly oxidized (photo) products that have yet to be identified. However, 4,6-dihydroxypyrimidine, where the second oxygen atom would be added to the ring in position 6 (Fig. 10), was not detected in our samples.

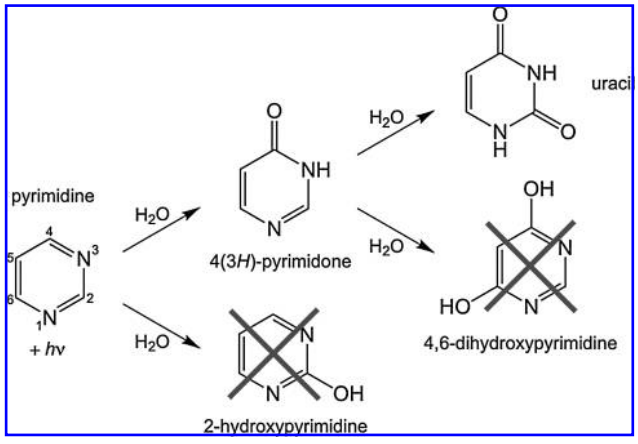

FIG. 10. Possible chemical pathway to the formation of uracil from the addition of oxygen atoms stemming from H_2O to pyrimidine. In such a regioselective mechanism, 4(3*H*)-pyrimidone is the first and major singly oxidized pyrimidine derivative formed (no 2-hydroxypyrimidine was detected in our samples), and uracil is the major (photo) product of 4(3*H*)-pyrimidone through the addition of a second oxygen atom to the aromatic ring. Doubly oxidized 4,6-dihydroxypyrimidine was not detected in the samples. The numbers around the structure of pyrimidine indicate the positions for the chemical nomenclature of its derivatives.

It is difficult to know at which point during the irradiation and subsequent warm-up 4(3*H*)-pyrimidone and uracil are formed. When analyzed by high-performance liquid chromatography (see Section 3.2), these compounds were observed after extraction of the residues with liquid H_2O, which indicates that they could be formed in the ice matrix either during the UV irradiation at 20–30 K by photoprocesses or during the warm-up to 220 K via thermal processes (such as radical recombination) or by hydrolysis after being dissolved in H_2O or during all these steps. However, the GC-MS chromatograms of the samples that were kept dry until they were derivatized verify the presence of uracil without exposure to liquid H_2O. Although this does not tell us whether 4(3*H*)-pyrimidone and uracil are formed at low temperature during the UV irradiation or during the warm-up to 220 K, it clearly indicates that such compounds can form under interstellar/cometary conditions and in the absence of liquid water. The presence of uracil in the residues produced from the irradiation of H_2O:pyrimidine ice mixtures at 120 K suggests that extremely low temperatures are not required to form the oxidized pyrimidines.

Little is known about the molecular mechanism of formation and intermediate species of these oxidized derivatives of pyrimidine. The relative insensitivity to temperature and wavelength observed in our experiments (see Section 4.1) suggests a radical chemistry, driven by the formation of H• and HO• readily produced by the photodecomposition of H_2O. Previous studies on the oxidation of various PAHs in pure H_2O ice suggest that the addition of oxygen atoms proceeds via a cation intermediate of the PAHs (Bernstein *et al.*, 2002b, 2007, and references therein). Since pyrimidine is a six-atom aromatic ring like the molecular pattern repeated in PAHs, it is reasonable to consider the possibility that the oxidation of pyrimidine proceeds via a similar cationic state. The presence of nitrogen atoms may, however, modify the electronic density of the π electrons around the aromatic ring due to the polarized CN bonds and favor certain molecular positions on the pyrimidine molecule for the oxidation. This is in agreement with the compounds found in our residues, where the first oxygen atom appears to be primarily added to position 4 to form 4(3*H*)-pyrimidone and not to position 2 to form 2-hydroxypyrimidine and where the addition of a second oxygen atom favors the formation of uracil versus 4,6-dihydroxypyrimidine (Fig. 10).

4.3. Astrobiological implications

According to the molecular yields calculated for 4(3*H*)-pyrimidone and uracil in our sample, and compared with the

upper limits for the column densities of interstellar pyrimidine in the gas phase of $1.7–3.4\times10^{14}\,cm^{-2}$ derived from astronomical observations (Kuan *et al.*, 2003), the expected maximum column densities for 4(3*H*)-pyrimidone and uracil that form from the UV photo-irradiation of pyrimidine and may be released into the gas phase of molecular clouds are of the orders of 10^{11} and 10^{10} cm^{-2}, respectively. Such small abundances render their detection very difficult even with the use of modern astronomical observatories. Of course, these column densities do not take into account the fact that oxidized pyrimidines, including 4(3*H*)-pyrimidone and uracil, can also be formed via other processes (cosmic rays) or via other (photo)chemical pathways from other starting compounds in the icy mantles on the surface of cold interstellar grains.

Our experiments clearly show that pyrimidine is more stable against UV photodestruction when mixed within H_2O ice than when it is isolated (Peeters *et al.*, 2005), and its photoproducts are stable enough to survive at room temperature. The half-life derived for pyrimidine in H_2O ice in our study is such that this compound in H_2O would be preserved from interstellar, circumstellar, and cometary environments until its delivery to telluric planets. In addition, uracil is preserved in the final residues, suggesting that such complex prebiotic molecules could be formed under interstellar, circumstellar, or cometary conditions, be preserved in mixed ices, and eventually reach Earth. Uracil and other compounds of prebiotic interest could then be enhanced by chemical processes in small parent bodies (mainly comets and asteroids) or later at the surface of telluric planets or in primordial oceans.

This scenario is qualitatively consistent with the presence of oxidized pyrimidines in carbonaceous chondrites such as Murchison, Murray, and Orgueil. The detection of 4-hydroxypyrimidine, the tautomer of 4(3*H*)-pyrimidone, has been reported in these meteorites (Folsome *et al.*, 1971, 1973; Lawless *et al.*, 1972); and, to the best of our knowledge, no other singly oxidized pyrimidines have yet been reported in these meteorites. Uracil was also first tentatively detected in Murchison (Stoks and Schwartz, 1979), and its extraterrestrial origin was recently confirmed by isotopic measurements (Martins *et al.*, 2008). No other dihydroxypyrimidines, however, have yet been identified in meteorites. These results are consistent with our experiments where 4(3*H*)-pyrimidone and uracil are the major products of the addition of one and two oxygen atoms to pyrimidine, respectively, under astrophysically relevant conditions (see Section 4.2 and Fig. 10). However, the possibility that other oxidized photoproducts may be responsible for some of the unidentified peaks in the chromatograms (Figs. 4, 6, 7, and 9) is not to be ruled out. Indeed, in the GC-MS chromatograms, several peaks have been detected for the masses that correspond to the addition of one ($m/z = 153$ amu) and two oxygen atoms ($m/z = 283$ amu) to a molecule of pyrimidine (top and middle traces of Fig. 8, respectively).

In Murchison, 4-hydroxypyrimidine [*i.e.*, 4(3*H*)-pyrimidone] was found with abundances of $\sim 6\,\mu g$ per gram of meteorite (Folsome *et al.*, 1971), whereas uracil was detected with an abundance of $\sim 0.03\,\mu g$ per gram of meteorite (Stoks and Schwartz, 1979). Thus, uracil is more than two orders of magnitude less abundant in the meteorite than 4(3*H*)-pyrimidone, and the meteoritic uracil:4(3*H*)-pyrimidone ratio is about 20 times lower than in our residues.

There could be several causes for this difference if the formation of uracil and the formation of 4(3*H*)-pyrimidone have an origin in interstellar/protostellar ice photochemistry. First, and perhaps most obvious, is the possibility that the initial amounts of uracil and 4(3*H*)-pyrimidone have been subsequently altered by parent body processes that produced or destroyed either of these species in the meteorite. There are also reasons why uracil might be produced at lower abundances in real interstellar ices, where pyrimidine and its derivatives do not interact only with pure H_2O. CH_3OH, NH_3, CO, and CO_2 are also present, and these may lead to the formation of other molecules when pyrimidine and its oxidized derivatives are subjected to irradiation. In this case, a smaller fraction of 4(3*H*)-pyrimidone may be converted to uracil via oxidation, while some of the 4(3*H*)-pyrimidone could also be converted by addition of $-CH_3$, $-NH_2$, $-COOH$ groups, or any combination of these, which would result in the formation of additional species including the nucleobases thymine (*i.e.*, a methyl $-CH_3$ group added to a molecule of uracil in position 5) and cytosine (*i.e.*, a molecule of uracil where the oxygen atom at position 4 has been substituted by an amino $-NH_2$ group) (see Fig. 1). We are currently carrying out experiments where pyrimidine is mixed with other ices of astrophysical interest and UV photo-irradiated to study the production of these other possible photoproducts of pyrimidine.

5. Conclusions

Uracil was found in the residues formed from the UV photolysis of pyrimidine in pure H_2O ice by using high-performance liquid chromatography and gas chromatography–mass spectrometry techniques, with a derived molecular yield of 4×10^{-5}. Among the other identified oxidized photoproducts of H_2O and pyrimidine, 4(3*H*)-pyrimidone has been conclusively identified with a yield estimated to be 10 times higher than that of uracil. These two compounds are believed to form mostly in the icy bulk in the vacuum chamber, during the UV photo-irradiation of H_2O:pyrimidine ice mixtures and warm-up to 220 K. 2,2′-Bipyrimidine, as well as probably other bipyrimidine isomers, were also observed in the residues. HPLC and GC-MS data demonstrate that additional products are also made, some of which are likely to be other singly and doubly oxidized pyrimidine derivatives.

The relative insensitivity of the suite of the products to H_2O:pyrimidine starting ratio, ice temperature, and radiation field suggests that the formation of such organic molecules via abiotic processes in astrophysical environments may be efficient. Thus, it is possible that oxidized pyrimidines, in particular nucleobases such as uracil, can form in interstellar or cometary environments via nonbiological processes and without being in contact with liquid H_2O.

The observed survival of pyrimidine and its derivatives, which were embedded in pure H_2O ice and subjected to UV photons, along with the presence of compounds of this type in meteorites, suggests that such compounds can be preserved from the astrophysical environments where they are likely to form, incorporated into asteroids and comets during the formation of the solar nebula, and subsequently delivered to telluric planets such as Earth.

Experiments in which pyrimidine is mixed with other ices of astrophysical interest (ices containing NH_3, CH_3OH, CO,

CO_2) and UV photo-irradiated under similar conditions are currently being carried out for comparison with the results described here.

Acknowledgments

This work was supported by NASA grants from the "Astrobiology" and "Origins of Solar Systems" programs. M.N., S.N.M., and S.A.S. would also like to acknowledge excellent technical support from R. Walker and thank M. Levit for his contribution to the preparation of the samples and standards for high-performance liquid chromatography analysis.

Author Disclosure Statement

No competing financial interests exist.

Abbreviations

amu, atomic mass units; GC-MS, gas chromatograph–mass spectrometer; HPLC, high-performance liquid chromatograph; ISM, interstellar medium; m/z, mass-to-unit charge ratio; PAHs, polycyclic aromatic hydrocarbons; PANHs, polycyclic aromatic nitrogen heterocycles.

References

Allamandola, L.J., Sandford, S.A., and Valero, G.J. (1988) Photochemical and thermal evolution of interstellar/precometary ice analogs. *Icarus* 76:225–252.

Allamandola, L.J., Tielens, A.G.G.M., and Barker, J.R. (1989) Interstellar polycyclic aromatic hydrocarbons—the infrared emission bands, the excitation/emission mechanism, and the astrophysical implications. *Astrophys. J., Suppl. Ser.* 71:733–775.

Ashbourn, S.F.M., Elsila, J.E., Dworkin, J.P., Bernstein, M.P., Sandford, S.A., and Allamandola, L.J. (2007) Ultraviolet photolysis of anthracene in H_2O interstellar ice analogs: potential connection to meteoritic organics. *Meteorit. Planet. Sci.* 42:2035–2041.

Bernstein, M.P., Sandford, S.A., Allamandola, L.J., Chang, S., and Scharberg, M.A. (1995) Organic compounds produced by photolysis of realistic interstellar and cometary ice analogs containing methanol. *Astrophys. J.* 454:327–344.

Bernstein, M.P., Sandford, S.A., and Allamandola, L.J. (1997) The infrared spectra of nitriles and related compounds frozen in Ar and H_2O. *Astrophys. J.* 476:932–942.

Bernstein, M.P., Sandford, S.A., Allamandola, L.J., Gillette, J.S., Clemett, S.J., and Zare, R.N. (1999) UV irradiation of polycyclic aromatic hydrocarbons in ices: production of alcohols, quinones, and ethers. *Science* 283:1135–1138.

Bernstein, M.P., Dworkin, J.P., Sandford, S.A., and Allamandola, L.J. (2001) Ultraviolet irradiation of naphthalene in H_2O ice: implications for meteorites and biogenesis. *Meteorit. Planet. Sci.* 36:351–358.

Bernstein, M.P., Dworkin, J.P., Sandford, S.A., Cooper, G.W., and Allamandola, L.J. (2002a) The formation of racemic amino acids by ultraviolet photolysis of interstellar ice analogs. *Nature* 416:401–403.

Bernstein, M.P., Elsila, J.E., Dworkin, J.P., Sandford, S.A., Allamandola, L.J., and Zare, R.N. (2002b) Side group addition to the PAH coronene by UV photolysis in cosmic ice analogs. *Astrophys. J.* 576:1115–1120.

Bernstein, M.P., Moore, M.H., Elsila, J.E., Sandford, S.A., Allamandola, L.J., and Zare, R.N. (2003) Side group addition to the PAH coronene by proton irradiation in cosmic ice analogs. *Astrophys. J.* 582:L25–L29.

Bernstein, M.P., Sandford, S.A., and Allamandola, L.J. (2005) The mid-infrared absorption spectra of neutral polycyclic aromatic hydrocarbons in conditions relevant to dense interstellar clouds. *Astrophys. J., Suppl. Ser.* 161:53–64.

Bernstein, M.P., Sandford, S.A., Mattioda, A.L., and Allamandola, L.J. (2007) Near- and mid-infrared laboratory spectra of PAH cations in solid H_2O. *Astrophys. J.* 664:1264–1272.

Casal, S., Mendes, E., Fernandes, J.O., Oliveira, M.B.P.P., and Ferreira, M.A. (2004) Analysis of heterocyclic aromatic amines in foods by gas chromatography–mass spectrometry as their *tert.*-butyldimethylsilyl derivatives. *J. Chromatogr. A* 1040:105–114.

Charnley, S.B., Kuan, Y.-J., Huang, H.-C., Botta, O., Butner, H.M., Cox, N., Despois, D., Ehrenfreund, P., Kisiel, Z., Lee, Y.-Y., Markwick, A.J., Peeters, Z., and Rodgers, S.D. (2005) Astronomical searches for nitrogen heterocycles. *Adv. Space Res.* 36:137–145.

Cottin, H., Moore, M.H., and Bénilan, Y. (2003) Photodestruction of relevant interstellar molecules in ice mixtures. *Astrophys. J.* 590:874–881.

Demyk, K., Dartois, E., d'Hendecourt, L., Jourdain de Muizon, M., Heras, A.M., and Breitfellner, M. (1998) Laboratory identification of the 4.62 μm solid state absorption band in the ISO-SWS spectrum of RAFGL 7009S. *Astron. Astrophys.* 339:553–560.

Destexhe, A., Smets, J., Adamowicz, L., and Maew, G. (1994) Matrix isolation FT-IR studies and *ab initio* calculations of hydrogen-bonded complexes of molecules modeling cytosine or isocytosine tautomers. 1. Pyridine and pyrimidine complexes with H_2O in Ar matrices. *J. Phys. Chem.* 98:1506–1514.

Elsila, J.E., Hammond, M.R., Bernstein, M.P., Sandford, S.A., and Zare, R.N. (2006) UV photolysis of quinoline in interstellar ice analogs. *Meteorit. Planet. Sci.* 41:785–796.

Elsila, J.E., Dworkin, J.P., Bernstein, M.P., Martin, M.P., and Sandford, S.A. (2007) Mechanisms of amino acid formation in interstellar ice analogs. *Astrophys. J.* 660:911–918.

Folsome, C.E., Lawless, J., Romiez, M., and Ponnamperuma, C. (1971) Heterocyclic compounds indigenous to the Murchison meteorite. *Nature* 232:108–109.

Folsome, C.E., Lawless, J., Romiez, M., and Ponnamperuma, C. (1973) Heterocyclic compounds recovered from carbonaceous chondrites. *Geochim. Cosmochim. Acta* 37:455–465.

Gaigeot, M.-P. and Sprik, M. (2003) *Ab initio* molecular dynamics computation of the infrared spectrum of aqueous uracil. *J. Phys. Chem. B* 107:10344–10358.

Galliano, F., Madden, S.C., Tielens, A.G.G.M., Peeters, E., and Jones, A.P. (2008) Variations of the mid-IR aromatic features inside and among galaxies. *Astrophys. J.* 679:310–345.

Gerakines, P.A., Moore, M.H., and Hudson, R.L. (2001) Energetic processing of laboratory ice analogs: UV photolysis versus ion bombardment. *J. Geophys. Res.* 106:33381–33386.

Hayatsu, R. (1964) Orgueil meteorite: organic nitrogen contents. *Science* 146:1291–1293.

Hayatsu, R., Anders, E., Studier, M.H., and Moore, L.P. (1975) Purines and triazines in the Murchison meteorite. *Geochim. Cosmochim. Acta* 39:471–488.

Hudgins, D.M., Sandford, S.A., Allamandola, L.J., and Tielens, A.G.G.M. (1993) Mid- and far-infrared spectroscopy of ices—

optical constants and integrated absorbances. *Astrophys. J. Suppl. Ser.* 86:713–870.

Kuan, Y-J., Yan, C.-H., Charnley, S.B., Kisiel, Z., Ehrenfreund, P., and Huang, H.-C. (2003) A search for interstellar pyrimidine. *Month. Not. R. Astron. Soc.* 345:650–656.

Kuan, Y.-J., Charnley, S.B., Huang, H.-C., Kisiel, Z., Ehrenfreund, P., Tseng, W.-L., and Yan, C.-H. (2004) Searches for interstellar molecules of potential prebiotic importance. *Adv. Space Res.* 33:31–39.

Lacy, J.H., Baas, F., Allamandola, L.J., van de Bult, C.E.P., Persson, S.E., McGregor, P.J., Lonsdale, C.J., and Geballe, T.R. (1984) 4.6 micron absorption features due to solid phase CO and cyano group molecules toward compact infrared sources. *Astrophys. J.* 276:533–543.

Lawless, J.G., Folsome, C.E., and Kvenvolden, K.A. (1972) Organic matter in meteorites. *Sci. Am.* 226:38–46.

MacKenzie, S.L., Tenaschuk, D., and Fortier, G. (1987) Analysis of amino acids by gas-liquid chromatography as *tert*-butyldimethylsilyl derivatives: preparation of derivatives in a single reaction. *J. Chromatogr. A* 387:241–253.

Martins, Z., Botta, O., Fogel, M.L., Sephton, M.A., Glavin, D.P., Watson, J.S., Dworkin, J.P., Schwartz, A.W., and Ehrenfreund, P. (2008) Extraterrestrial nucleobases in the Murchison meteorite. *Earth Planet. Sci. Lett.* 270:130–136.

Mathis, J.S., Mezger, P.G., and Panagia, N. (1983) Interstellar radiation field and dust temperatures in the diffuse interstellar matter and in giant molecular clouds. *Astron. Astrophys.* 128:212–229.

Muñoz Caro, G.M. and Schutte, W.A. (2003) UV-photoprocessing of interstellar ice analogs: new infrared spectroscopic results. *Astron. Astrophys.* 412:121–132.

Nuevo, M., Auger, G., Blanot, D., and d'Hendecourt, L. (2008) A detailed study of the amino acids produced from the vacuum UV irradiation of interstellar ice analogs. *Orig. Life Evol. Biosph.* 38:37–56.

Palumbo, M.E., Pendleton, Y.J., and Strazzulla, G. (2000) Hydrogen isotopic substitution studies of the 2165 wavenumber (4.62 micron) "XCN" feature produced by ion bombardment. *Astrophys. J.* 542:890–893.

Peeters, Z., Botta, O., Charnley, S.B., Kisiel, Z., Kuan, Y.-J., and Ehrenfreund, P. (2005) Formation and photostability of *N*-heterocycles in space. I. The effect of nitrogen on the photostability of small aromatic molecules. *Astron. Astrophys.* 433: 583–590.

Prasad, S.S. and Tarafdar, S.P. (1983) UV radiation field inside dense clouds—its possible existence and chemical implications. *Astrophys. J.* 267:603–609.

Puget, J.L. and Léger, A. (1989) A new component of the interstellar matter: small grains and large aromatic molecules. *Annu. Rev. Astron. Astrophys.* 27:161–198.

Ricca, A., Bauschlicher, C.W., and Bakes, E.L.O. (2001) A computational study of the mechanisms for the incorporation of a nitrogen atom into polycyclic aromatic hydrocarbons in the Titan haze. *Icarus* 154:516–521.

Roelfsema, P.R., Cox, P., Tielens, A.G.G.M., Allamandola, L.J., Baluteau, J.P., Barlow, M.J., Beintema, D., Boxhoorn, D.R., Cassinelli, J.P., Caux, E., Churchwell, E., Clegg, P.E., de Graauw, T., Heras, A.M., Huygen, R., van der Hucht, K.A., Hudgins, D.M., Kessler, M.F., Lim, T., and Sandford, S.A. (1996) SWS observations of IR emission features towards compact HII regions. *Astron. Astrophys.* 315:L289–L292.

Sandford, S.A. and Allamandola, L.J. (1990) The physical and infrared spectral properties of CO_2 in astrophysical ice analogs. *Astrophys. J.* 355:357–372.

Sandford, S.A., Allamandola, L.J., Tielens, A.G.G.M., and Valero, G.J. (1988) Laboratory study of the infrared spectral properties of CO in astrophysical ices. *Astrophys. J.* 329:498–510.

Sandford, S.A., Bernstein, M.P., and Allamandola, L.J. (2004) The mid-infrared laboratory spectra of naphthalene ($C_{10}H_8$) in solid H_2O. *Astrophys. J.* 607:346–360.

Schutte, W.A. and Greenberg, J.M. (1997) Further evidence for the OCN^- assignment to the XCN band in astrophysical ice analogs. *Astron. Astrophys.* 317:L43–L46.

Shen, C.J., Greenberg, J.M., Schutte, W.A., and van Dishoeck, E.F. (2004) Cosmic ray induced explosive chemical desorption in dense clouds. *Astron. Astrophys.* 415:203–215.

Silverstein, R.M. and Bassler, G.C. (1967) *Spectrometric Identification of Organic Compounds,* 2nd ed., John Wiley and Sons, New York.

Simon, M.N. and Simon, M. (1973) Search for interstellar acrylonitrile, pyrimidine, and pyridine. *Astrophys. J.* 184:757–762.

Stoks, P.G. and Schwartz, A.W. (1979) Uracil in carbonaceous meteorites. *Nature* 282:709–710.

Stoks, P.G. and Schwartz, A.W. (1981) Nitrogen-heterocyclic compounds in meteorites: significance and mechanisms of formation. *Geochim. Cosmochim. Acta* 45:563–569.

van der Velden, W. and Schwartz, A.W. (1977) Search for purines and pyrimidines in the Murchison meteorite. *Geochim. Cosmochim. Acta* 41:961–968.

Address correspondence to:
Michel Nuevo
NASA Ames Research Center
Space Science Division
Mail Stop 245-6
Moffett Field, CA 94035
USA

E-mail: michel.nuevo-1@nasa.gov